

Effect of iron ionization balance on X-ray spectral analysis

K. Masai

Department of Physics, Tokyo Metropolitan University, Hachioji, Tokyo 192-03, Japan

Received 14 October 1996 / Accepted 29 January 1997

Abstract. We have investigated the uncertainty in the ionization and recombination rates for iron and its impact on the derivation of the iron elemental abundance from X-ray emission spectra. Most uncertainty is found in the dielectronic recombination rates for iron ions with L-shell outer electrons. The quantitative effect of this uncertainty on the derivation of the iron abundance depends on the spectral resolving power of X-ray detectors. With the resolution achieved by *ASCA*, the differences among ionization balance models come out to $\sim 30\%$ in the iron elemental abundance and $\sim 15\%$ in the temperature at temperatures $kT \sim 1$ keV. To eliminate the effects of the ionization balance, finally, we suggest taking ionization temperature as well as the electron temperature into account for spectral analysis. This way is useful also for plasmas in the presence of ionizing photons.

Key words: atomic and molecular processes – plasmas – X-rays: general

1. Introduction

The amount of iron has been of special interest in various classes of astrophysical objects with respect to their evolution. In a cluster of galaxies, the iron abundance today in the intracluster medium tells a history of star formation in the galaxies, nucleosynthesis in the stars, and the circulation through supernova explosions or galactic winds. The medium on the order of 10^7 K emits soft X-rays with iron lines, and the iron abundance can be determined by the spectral analysis. The hot intracluster gas is so tenuous as to attain coronal conditions for atomic level populations and is optically thin to the resultant emission lines. Then, the line emission comes out as a product of the specific emissivity, ionic fraction and elemental abundance integrated over the line of sight. The specific emissivity, the emissivity per ion-electron pair, is a function of the electron temperature, and ionization is driven by electron impact in such a tenuous and optically thin medium. Therefore, if the medium is in ionization equilibrium, the emissivity per iron atom must be a function simply of the electron temperature. Hence, the elemental abundance can be obtained primarily by determining the temperature of the medium from the emission spectrum.

Even in such a simple case of coronal equilibrium, however, we need to define two processes, ionic fraction (ionization-recombination balance) and the specific emissivity. Spectral analysis of *ASCA* data has raised questions about the accuracy of plasma emission codes in use, and the related problems have been investigated (Brickhouse et al. 1995; Mewe, Kaastra & Liedahl 1995). In relation to the analysis of clusters of galaxies observed by *Ginga*, Arnaud et al. (1991) compared the plasma radiation codes of Raymond & Smith (1977), Masai (1984) and Mewe et al. (1985). For the equivalent width of iron K-lines (Fig. 6 in their paper) they found that Raymond & Smith (1977) predicted lower values at $kT < 2$ keV and higher values at $kT > 2$ keV compared to the other two codes. Though the low values below 2 keV were partially due to lack of satellite lines that should be taken into account, the overall difference could be ascribed to a difference in the ionization balance. In the *Ginga* observations, the iron analysis was restricted to its K-shell lines, which, with the resolving power of *Ginga*, could be isolated from lines of other major elements except for nickel. The atomic processes involved with K-lines are less uncertain than those with the L-lines. The higher resolving power of *ASCA* allows and requires to analyze iron L-lines as well, which are blended complicatedly with many lines of other elements. We have investigated the atomic processes responsible for iron L-line emission and its implications for spectral analysis.

The present paper is focused on the uncertainty in the ionization-recombination process, which is a basis to evaluate the specific emissivity. In the following section, we compare the iron ionization balance calculated in our radiation code (Masai 1984) with those given by the ionization and recombination rates recommended by Arnaud & Rothenflug (1985) and Arnaud & Raymond (1992). In Sect. 3, we show the influence of the iron ionization balance on spectral analysis, intending to simulate a case with a spectral resolving power as achieved by *ASCA* (Tanaka, Inoue & Holt 1994). We compare the spectra with the three sets of ionization and recombination rates, and discuss which atomic process is most important for the determination of the iron elemental abundance in spectral analysis. We also consider a case of higher resolving power as achieved by a crystal spectrometer. As a reference we analyze the solar flare data obtained by SOLEX A (McKenzie et al. 1980) with the three sets of atomic rates. Finally, we discuss some ideas to

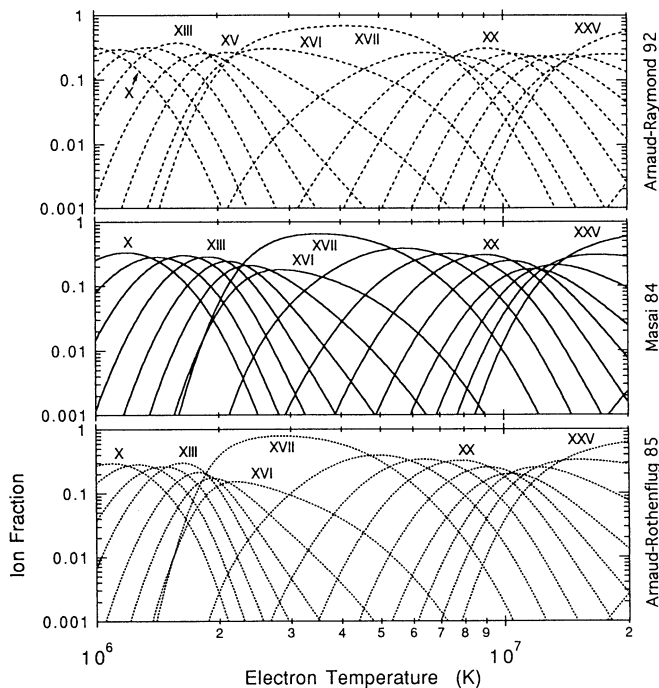


Fig. 1. Iron ion fraction as a function of electron temperature for three collisional ionization models indicated on the right.

obtain as reliable elemental abundance as possible and to qualify the theoretical atomic rates from the comparison with the observations.

2. Ionization balance

For the elements of major astrophysical interest, a data set of ionization and recombination rates has been compiled by Arnaud & Rothenflug (1985). This data set was used by Mewe et al. (1985) to calculate radiation spectra in their computer code. Later, Arnaud & Raymond (1992) gave recommended data for iron based on recent atomic calculations. On the other hand, various atomic data have been compiled and evaluated by Kato and her colleagues at the Institute of Plasma Physics, Nagoya (e.g., see Kato, Masai & Arnaud 1991), and have been applied to calculate radiation spectra since Masai (1984). For the iron ionization balance, this data set gives an intermediate result between the later two publications, Arnaud-Rothenflug 85 and Arnaud-Raymond 92. The iron ionization balance calculated with these three data sets is compared in Fig. 1. As demonstrated later, there is no significant difference for elements lighter than iron between Masai 84 and Arnaud-Rothenflug 85; note that Arnaud-Raymond 92 gave data only for iron. From a comparison of Arnaud-Raymond 92 and Arnaud-Rothenflug 85, we see that the most drastic change was made for the ionic states around Ne-like iron (Fe XVII).

We are looking into detail to each atomic process responsible for the ionization balance. Direct and auto-ionization rates for iron were not changed appreciably from Arnaud-Rothenflug 85 to Arnaud-Raymond 92, and the total rates are fairly in good

agreement with Masai 84 in the temperature range of practical interest (Kato, Masai & Arnaud 1992). The radiative recombination rates also show a good agreement (Kato & Masai 1991, unpublished). Finally, we have found the strongest differences in the effective dielectronic recombination rates. In this process, electron capture does not produce a photon but it excites a bound electron, resulting in a doubly excited state. This state is stabilized by the following autoionization or radiative transition. The latter process produces a dielectronic recombination satellite line. If autoionization dominates, no actual recombination occurs eventually. Therefore, the autoionization rate significantly affects the total recombination rate and the resultant ionization balance.

Since Jacobs et al. (1977) pointed out an important role for autoionization in the dielectronic recombination process, various theoretical calculations have been carried out for this topic. However, it seems that the results have not yet converged. In fact, many results at the publication date of Arnaud & Rothenflug (1985) suggested higher autoionization rates than those by Jacobs et al. (1977), but in turn lower rates these years as adopted by Arnaud-Raymond 92. As a result, Arnaud-Raymond 92 has the Ne-like iron fraction rising slowly and covering a wider range of temperature than Arnaud-Rothenflug 85. The distribution of Arnaud-Raymond 92 looks more similar to that of Jordan (1969), which was proposed several years before the Jacobs' claim.

Arnaud-Raymond 92 rates are based on the latest theoretical calculations. From an aspect of electronic sequence consistency, however, there are some questions left. For instance, as seen in Fig. 1, this data set shows that Na-like iron (Fe XVI) reaches a maximum fraction larger than that of Mg-like (Fe XV) or F-like (Fe XVIII). It is reasonable that Na-like is outstanding because of its closed principal shell, but we cannot find a simple explanation for Na-like to be so stable as suggested by Arnaud-Raymond 92. Another question is why N-like (Fe XX) looks more stable or reaches a maximum fraction larger than its neighbors, O-like and C-like despite that the ionization potential varies smoothly with the ionic state in this range. The same situation is also found in Si-like (Fe XIII) and its neighbors.

3. Emission spectra

It is of astrophysical interest to know how the different ionization balances give different results for quantities like the temperature, emission measure, elemental abundances, and so on. In order to illustrate this, we compare the spectral emissivity predicted by the three data sets of ionization and recombination rates. For all cases hereafter, the same spectral code (Masai 1984, 1994b) is used to calculate the specific emissivity. For the elemental abundances, the solar values by Allen (1973) are used if not specifically mentioned. Fig. 2 shows the spectral emissivity per hydrogen atom as a function of electron temperature. Except for iron, Arnaud-Raymond 92 rates are the same as Arnaud-Rothenflug 85 and are in good agreement with Masai 84. The uncertainty in the iron data corresponds to a difference

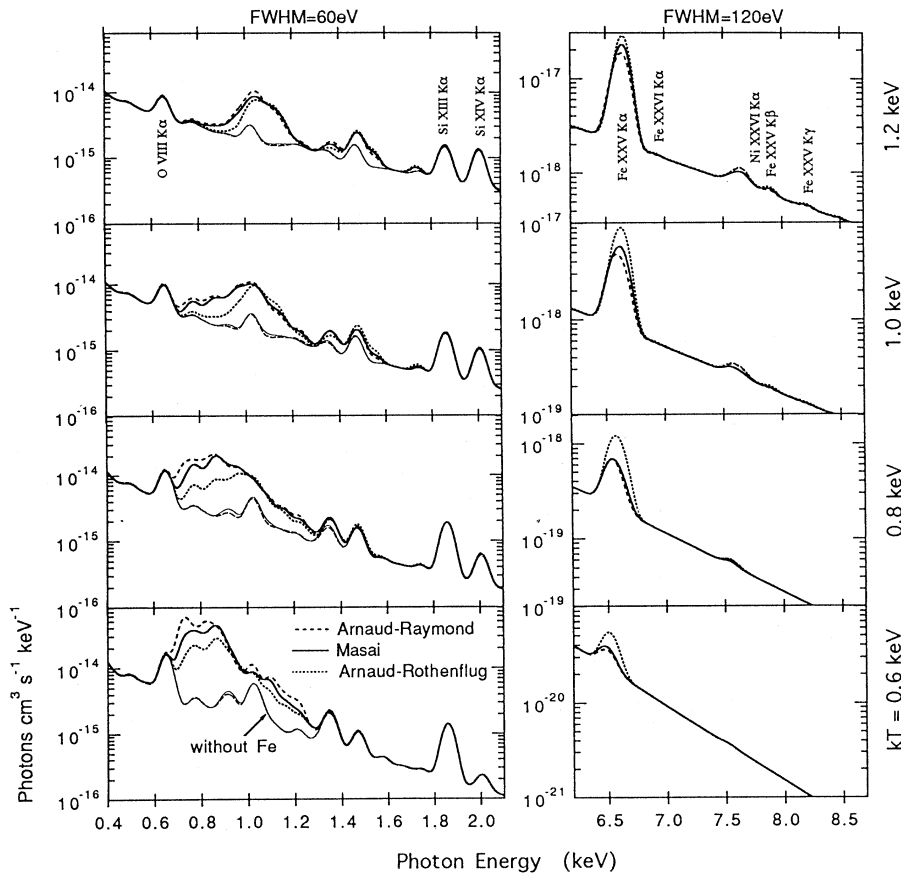


Fig. 2. Spectral emissivity at electron temperatures, $kT = 0.6, 0.8, 1.0$ and 1.2 keV, for three ionization models. The spectra are convolved with Gaussian kernels with FWHM = 60 and 120 eV for the low and high energy bands, respectively. The thin lines represent the case without iron.

of a factor of 2 or more in the spectral emissivity at a temperature below 1 keV.

Since a different ionization balance predicts a different temperature, the comparison of the emissivity at a given temperature does not immediately give the difference in the elemental abundance to be derived. In order to see the practical effect on the abundance determination, we simulated spectra in such a way as shown in Fig. 3. Here we calculated a target spectrum at 1 keV with normal (Allen 1973) iron abundance using the Masai 84 code, and tried to reproduce it using the other two data sets with temperature and iron abundance being free parameters. From this figure we see that Arnaud-Rothenflug 85 and Arnaud-Raymond 92 predict a 0.7 times and 0.9 times, respectively, smaller iron abundance than Masai 84. In Arnaud-Rothenflug 85, also the oxygen abundance and the Si H/He-like ratio must be tuned to get a better fit, since the predicted temperature is lower than the others. The smaller iron abundance and the lower temperature predicted by this data set is likely systematic at temperatures below 1 keV, while no such tendency is found in Arnaud-Raymond 92.

To see the influence on highly resolved spectra, we analyzed the solar flare spectra observed from SOLEXA on 10 June, 1979. Fig. 4 shows the data taken from Table 1 in McKenzie et al. (1980): from the top to the bottom, the raw peak counts, the flux after corrections, and their ratio are plotted for each spectral line in the wavelength region from 10 to 19 Å. The broken line superposed on the flux/counts ratio represents a least square

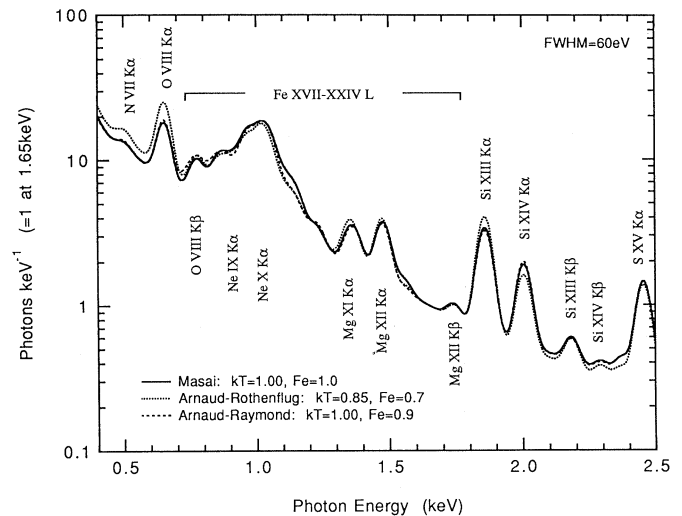


Fig. 3. Simulation of the role of the practical effect of ionization balance on the spectral analysis of ASCA data: a spectrum calculated with MASAI 84 is analyzed by using the other two models with electron temperature and iron elemental abundance being free parameters. See text.

fit to it, and is used to make a correction for the wavelength-dependent efficiency of the detector. The jump across 18.09 Å is due to the fluorine K edge of the detector material (MgF_2 photocathode). This leap is estimated from the flux/counts ratio

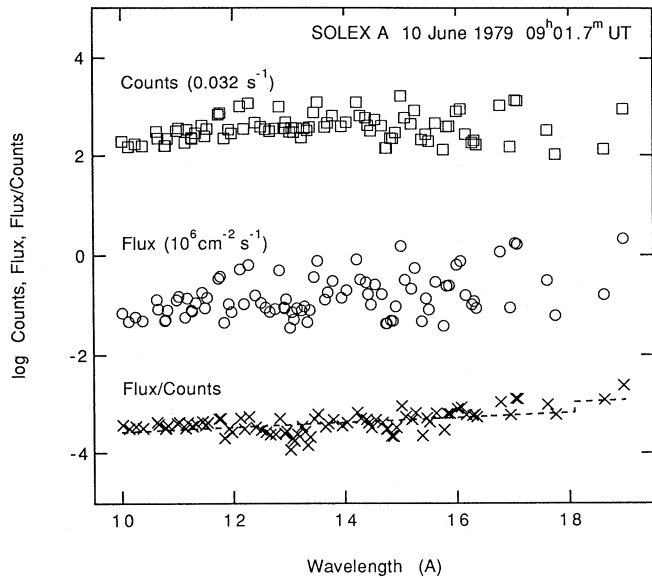


Fig. 4. Solar flare data observed from SOLEX A. The broken line represents the correction curve obtained from the Flux/Counts ratio.

of prominent lines shorter than this edge to that of the O VIII resonance line at 18.97 Å.

Using the correction factor (the broken line in Fig. 4), we reproduced the spectrum recorded from 08^h50^m5 UT after the transient phase. Several lines of Fe XVII and XVIII, and O VIII are prominent in the wavelength region from 13.6 to 19.2 Å, as shown in Fig. 5. Three of them, Fe XVIII $2p^2P_{3/2}-3d^2D_{5/2}$ (14.22 Å), Fe XVII $2p^1S_0-3d^3D_1$ (15.26 Å) and Fe XVIII $2p^2P_{3/2}-3s^4P_{5/2}$ (16.07 Å) are sensitive to the temperature, and their relative intensities give a good temperature estimate. For Arnaud-Rothenflug 85, Masai 84 and Arnaud-Raymond 92, we obtain temperatures around $4.5 \cdot 10^6$ K, $5 \cdot 10^6$ K and $7 \cdot 10^6$ K, respectively. As seen in Fig. 5, for these temperatures, also the weaker lines between 14.22 Å and 16.07 Å are well reproduced with the line data in the Masai code. We take into account about 100 lines of Ni, O, Ne, Ca, Fe and Ni as well as continuum in the same manner as in Figs. 2 and 3. For the simulated spectra in Fig. 5, we assume a FWHM of a line of 0.3 Å.

Once the temperature is determined by the three key lines, Fe XVII 15.26 Å and XVIII 14.22 Å and 16.07 Å, attention must be paid to the relative intensities of the strongest Fe XVII resonance line $2p^1P-3d^1P$ (15.01 Å), $2p^1S-3s^1P$ (16.78 Å) and two $2p^1S-3s^3P$ (17.04 and 17.08 Å) of Fe XVII, and O VIII Ly α $1s^2S-2p^2P$ (18.97 Å). The four lines of Fe XVII of the same ionic state give a means to check the ionization balance relative to the specific emissivity. Their relative intensities depend on the temperature at which the ionization balance is realized to account for the three key lines of Fe XVII and XVIII. In comparison with SOLEX A data, the temperature suggested by Arnaud-Raymond 92 may be too high to account for the four lines of Fe XVII consistently. On the other hand, the relative intensities of the Fe XVII lines to the O VIII resonance line give a means to check the iron ionization balance relative to oxygen.

Arnaud-Rothenflug 85 and Arnaud-Raymond 92 give weaker and stronger iron line intensities, respectively, relative to their oxygen ionization balance values. Since the ionization and recombination rates for oxygen are the same in the two data sets, Arnaud-Rothenflug 85 and Arnaud-Raymond 92 could derive higher and lower, respectively, iron elemental abundance relative to oxygen. This result is consistent with the case in Fig. 3, where Arnaud-Rothenflug 85 yields a lower elemental abundance of oxygen compared to iron.

In the comparison here, we have assumed for simplicity that the plasma has a single temperature and chemical composition, and is free from transient conditions. In addition, our emissivity code is not always perfect. However, we see that other lower intensity lines than mentioned here are also quite well reproduced except for the blended lines of O VIII $1s^2S-3p^2P$ and Fe XVIII $2p^2P_{3/2}-3s^4P_{3/2}$ around 16 Å. The SOLEX A data were analyzed also by Cornille et al. (1994) for the same wavelength range. They applied the Arnaud-Raymond 92 ionization balance with a more sophisticated treatment of line emission. They assumed two temperature components, $2.5 \cdot 10^6$ K for Fe XVII and O VIII, and $5 \cdot 10^6$ K for Fe XVIII. However, they could not reproduce the observed relative intensities very well. A better fit was obtained by multiplying their theoretical excitation rates by 0.8 and 0.2 for O VIII and Fe XVIII, respectively. Their result may imply that there is something wrong in the ionization balance of iron relative to that of oxygen around the given temperatures, yet the iron lines could come from an emission region different from that of the oxygen lines.

4. Discussions

In the calculations as presented here, the ionization balance is our major interest, and the effects of nonequilibrium ionization have not been discussed. As described in Sect. 2, the most serious problem are the dielectronic recombination rates. When a plasma is ionizing, as observed in young supernova remnants, this is not very significant because the ionization state is ruled by ionization rates except for the asymptotic phase toward equilibrium. In another extreme case that the plasma is recombining, like e.g. a photoionized gas, the differences can be ignored because dielectronic recombination is suppressed under the condition that the electron temperature is quite low compared to the ionization degree or the ionization potential. Consequently, the issue of dielectronic recombination becomes serious only for plasmas around collisional ionization equilibrium.

With any choice of ionization and recombination rates, a better-look fit to observed spectra can be obtained by taking into account a deviation from equilibrium. The deviation may not always be physically real, however. Since the emissivity as well as the ionization balance is a function of the temperature, a spectral analysis would suggest a shift of the ionization balance relatively to the emissivity scale if they cannot consistently reproduce the spectrum at a given temperature. This situation is demonstrated already in Fig. 3 and now in Fig. 6 for a wider temperature range; the upper panel shows the emissivity integrated over the 0.6-1.8 keV band as a function of the electron temper-

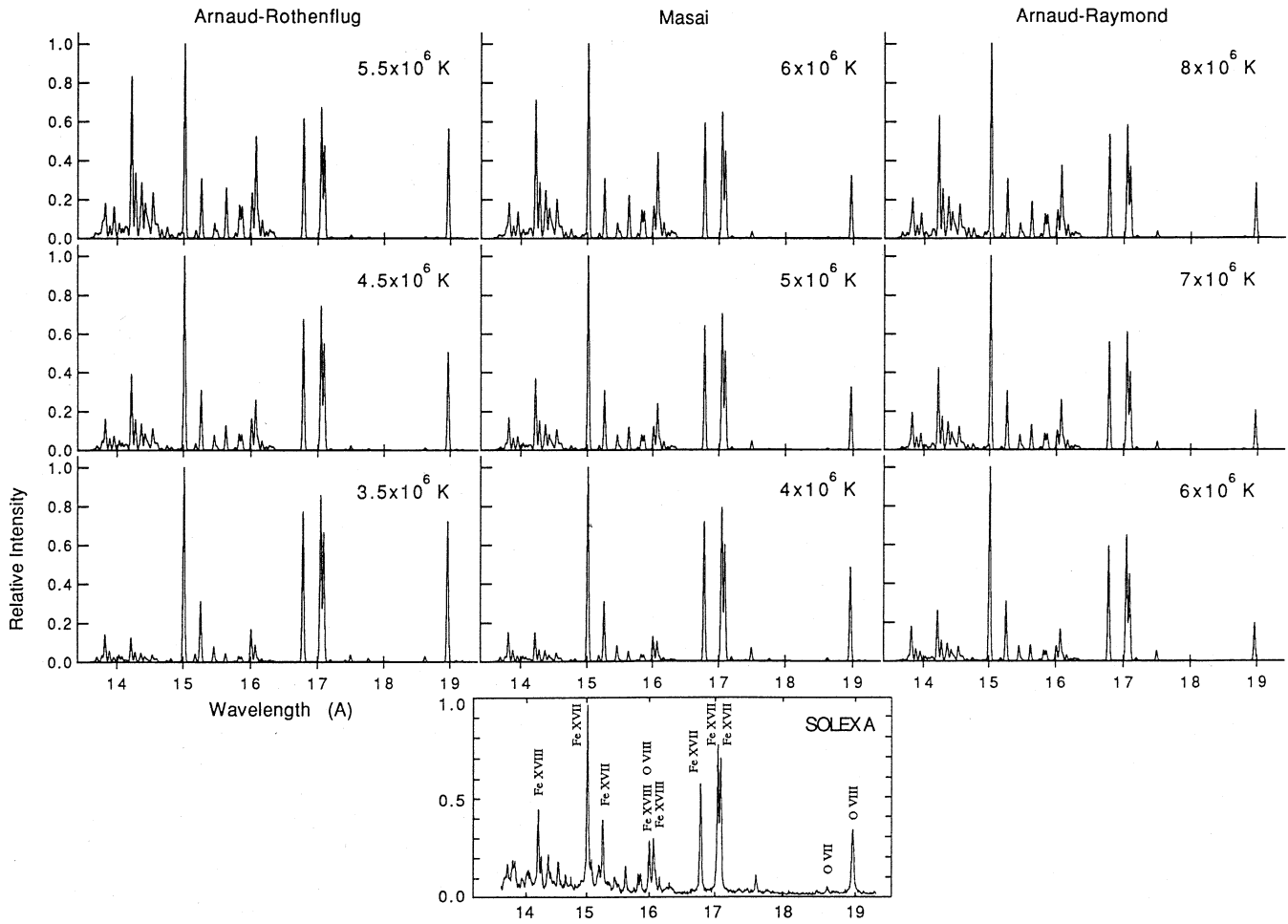


Fig. 5. Solar flare spectrum observed from SOLEX A and the reproduced spectra with three ionization models.

ature, and the lower one shows that as a function of the average ionic state of iron. Also shown in Fig. 6b is the temperature as a function of iron ionic state. From Fig. 6a one can see that the emissivity takes its maximum at a different temperature depending on the ionization and recombination rates. The maximum emissivity reached is lower and higher in Arnaud-Rothenflug 85 and Arnaud-Raymond 92, respectively, than Masai 84. This behavior is explained as follows in relation to the predicted ionization balance. When a plasma is in collisional ionization equilibrium, the line emissivity is dominated by electron-impact excitation. The excitation rate coefficient from level i to j can be written in a form

$$C_{ij} \propto G_{ij} T_e^{-(1/2+\alpha_{ij})} e^{-E_{ij}/kT_e},$$

where $G_{ij} \equiv G(kT_e/E_{ij})$ is the Gaunt factor averaged over a Maxwellian distribution, E_{ij} is the excitation energy, and α_{ij} is a parameter less than unity dependent on the oscillator strength of the transition; generally $\alpha \approx 0$ and $\alpha > 0$ for E1 and non E1 transitions, respectively (Masai 1994a). Since G_{ij} is weakly dependent on T_e , the rate coefficient reaches its maximum around

a temperature given by

$$kT_m \sim \frac{2}{1+2\alpha_{ij}} E_{ij}.$$

If G_{ij} is taken into account, kT_m may be a little bit higher than this value. In collisional ionization equilibrium, the ion fraction reaches its maximum and starts to decrease before the temperature reaches kT_m , because kT_m is higher than the ionization potential for $\Delta n \neq 0$ E1 transitions which fall in the X-ray band. Therefore, the emissivity becomes higher when the ion survives at higher temperatures ($\lesssim T_m$). As seen in Fig. 1 Arnaud-Rothenflug 85 and Arnaud-Raymond 92 predict a given ionization balance at lower and higher temperatures, and thus predict lower and higher emissivities, respectively.

Fig. 6a shows that the difference in the emissivity is significant in the range from $kT \sim 0.4$ to 1 keV where iron L-shell transitions dominate. Without iron, the three data sets give good agreement in the emissivity, as shown by the thin lines. This result is consistent with the lack of difference found in the rates for other elements, as discussed in Sect. 2. That is, the difference in the ionization balance of iron is the one relative to that of other elements. If we plot the emissivity as a function of iron

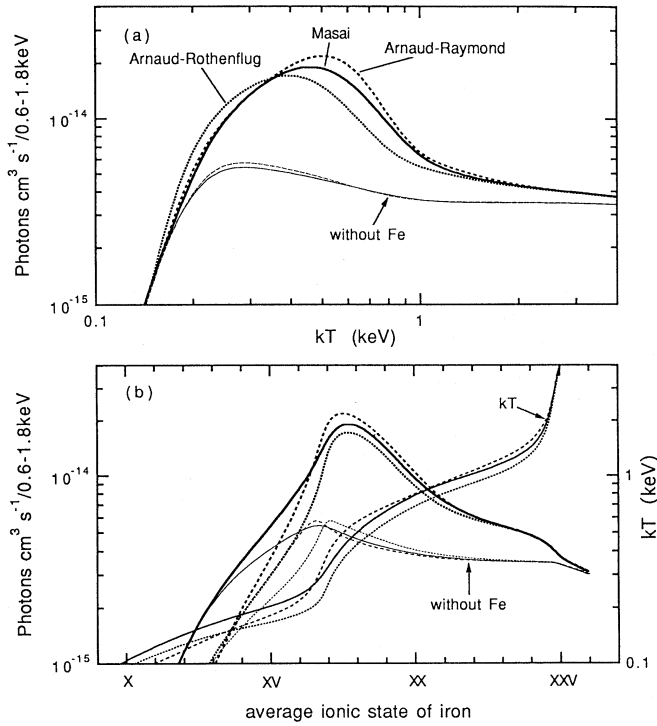


Fig. 6a and b. Integrated emissivity over 0.6-1.8 keV, where iron L-lines dominate, as a function of **a** electron temperature and **b** iron ionic state. In **b** the electron temperature is also shown as a function of iron ionic state. The thin lines represent the case without iron.

ionic state (Fig. 6b), the difference is reduced in the range where iron dominates, yet the difference is enhanced at $kT \lesssim 0.2$ keV where the contribution of other elements gets significant. This implies a possible way to isolate the effects of the ionization and recombination process from the emission process, i.e., the line data. In spectral analysis of observed spectra one can determine two temperatures, ionization temperature T_z and the usual electron temperature T_e ; $T_z < T_e$ for ionizing, $T_z > T_e$ for recombining, and $T_z \approx T_e$ for ionization equilibrium (Masai 1994b). In this context, T_z and T_e are related to the ionic state and the specific emissivity, respectively. In spectral analysis, if one of these three conditions holds consistently for all elements, the plasma is thought to be really in that condition. If iron shows either $T_z < T_e$ or $T_z > T_e$ although other elements consistently show $T_z \approx T_e$, there is likely something wrong in the ionization and recombination rates for iron. Such a result allows us to find a reasonable ionization balance of iron relative to those of other elements and the emissivity of iron itself, and to evaluate the atomic data concerned.

The above argument with T_z and T_e is applicable naturally for real nonequilibrium conditions. For ionizing plasmas such as young supernova remnants, analysis with $(n_e t, T_e)$ space has been widely applied (Masai 1984, 1994b). However, the $n_e t$ parameter is relevant for collisional processes, where the effective time for relaxation is proportional to the density. For a recombining condition occurring when ionizing photons are present, the analysis could indicate a value of $n_e t$ at a certain point on

its track to equilibrium, yet this value has no relation to collisional relaxation. In such a case, analysis with (T_z, T_e) space is more useful in order to reproduce the observed emission spectra and to understand the thermal structure of the plasma (Masai 1994b). Fig. 6b is an example of the (T_z, T_e) plane where the T_z scale is replaced by the iron ionic state.

5. Conclusions

We summarize the work on the iron ionization balance in the temperature range that is of practical importance for iron L-line spectral analysis.

1. The ionization balances of Arnaud-Rothenflug 85 and Masai 84 are in good agreement for the important elements except for iron. For iron Arnaud-Rothenflug 85 and Arnaud-Raymond 92 predict systematically higher and lower ionization states than Masai 84 at a given temperature.
2. There are no significant differences in the rates of ionization and radiative recombination for iron, but the dielectronic recombination rates differ. This issue becomes serious for plasmas around collisional ionization equilibrium.
3. The uncertainty in the iron ionization balance affects severely its L-shell lines which cannot be well isolated from lines of other major elements with resolving power as achieved by ASCA. Since the ionization balance responsible for K-lines is less uncertain, *Ginga* observations could derive iron abundance in fairly good agreement.
4. With a resolution of FWHM ~ 60 eV, the difference in the ionization balance between Arnaud-Rothenflug 85 and Arnaud-Raymond 92 results in a difference of more than a factor of two in the spectral emissivity in the range of photon energies 0.6-1.8 keV where iron L-lines dominate. This difference is pronounced at temperatures below $kT \sim 1$ keV.
5. The difference in the ionization balance causes a difference of at most 70% in the integrated 0.6-1.8 keV emissivity. This difference is most pronounced in the temperature range of $kT \sim 0.4$ -1 keV. The spectral emissivity or the integrated emissivity predicted by Masai 84 is between that of Arnaud-Rothenflug 85 and Arnaud-Raymond 92.
6. If we simulate a typical condition encountered in ASCA data analysis, we find that Arnaud-Rothenflug 85 and Arnaud-Raymond 92 derive 30% and 10% smaller iron abundances, respectively, at $kT \sim 1$ keV than Masai 84 from spectra in the photon energy range of 0.6-1.8 keV. Arnaud-Rothenflug 85 may also derive low temperatures compared to the other two.
7. In order to isolate the effects of the ionization balance, we suggest performing the spectral analysis in the (T_z, T_e) space, where T_z is the ionization temperature, a measure of the ionization state in units of the temperature. This analysis is compatible with $(n_e t, T_e)$ analysis for nonequilibrium ionization and covers a wider range of thermal structure including recombining conditions by the presence of ionizing photons.

8. With higher resolving power, the intensity ratio of Fe XVIII $2p^2P_{3/2}-3d^2D_{5/2}$ (14.22 Å), Fe XVII $2p^1S_0-3d^3D_1$ (15.26 Å) and Fe XVIII $2p^2P_{3/2}-3s^4P_{5/2}$ (16.07 Å) can be useful for the temperature diagnostics.

Acknowledgements. The author would like to thank N. Yamasaki, T. Kaho, K. Matsushita, Y. Fukazawa for discussion and their useful comments based on their analysis of ASCA data. This work has been supported by the Grant in Aid (07222211) for Scientific Research of the Ministry of Education, Science and Culture in Japan.

References

- Allen, C.W., 1973, *Astrophysical Quantities*, The Athlone Press, University of London
- Arnaud M., Rothenflug R., 1985, *A&AS* 60, 425
- Arnaud M., Lachize-Rey, M., Rothenflug R., Yamashita, K., Hattakade, I., 1991, *A&AS* 243, 56
- Arnaud M., Raymond J.C., 1992, *ApJ* 398, 394
- Brickhouse N., Edgar R., Kaastra J.S. et al., 1995, *Legacy* 6, 4
- Cornille M., Dubau J., Faucher P., Bely-Dubau F., Blancard C., 1994, *A&AS* 105, 77
- Jacobs V.L., Davis J., Kepple P.C., Blaha M., 1977, *ApJ* 211, 605
- Jordan C., 1970, *MNRAS* 148, 17
- Kato T., Masai K., Arnaud M., 1991, NIFS-DATA-14, *Nat. Inst. Fusion Sci.*, Nagoya
- Masai K., 1984, *Ap&SS* 98, 367
- Masai K., 1994a, *JQSRT* 51, 211
- Masai K., 1994b, *ApJ* 437, 770
- McKenzie D.L., Landecker P.B., Broussard R.M. et al., 1980, *ApJ* 241, 409
- Mewe R., Kaastra J.S., Liedahl D.A., 1995, *Legacy* 6, 16
- Mewe R., Gronenschild E.H.B.M., van den Oord G.H.J., 1985, *A&AS* 62, 197
- Raymond J.C., Smith B.W., 1977, *ApJS* 35, 419
- Tanaka Y., Inoue H., Holt S.S., 1994, *PASJ* 46, L37